Gain-assisted light guiding at the subwavelength scale in a hybrid dielectric-loaded surface plasmon polariton waveguide based on a metal nanorod

2013 J. Phys. D: Appl. Phys. 46 335102

(http://iopscience.iop.org/0022-3727/46/33/335102)

IOP Publishing Journal of Physics D: Applied Physics
J. Phys. D: Appl. Phys. **46** (2013) 335102 (7pp) doi:10.1088/0022-3727/46/33/335102

Gain-assisted light guiding at the subwavelength scale in a hybrid dielectric-loaded surface plasmon polariton waveguide based on a metal nanorod

Yusheng Bian[1], Zheng Zheng[1], Xin Zhao[1], Jing Xiao[1], Haitao Liu[1], Jiansheng Liu[1], Tao Zhou[2] and Jinsong Zhu[3]

[1] School of Electronic and Information Engineering, Beihang University, Beijing 100191, People's Republic of China
[2] Department of Physics, New Jersey Institute of Technology, Newark, NJ 07102, USA
[3] National Center for Nanoscience and Technology, No.11 Zhongguancun Beiyitiao, Beijing 100190, People's Republic of China

E-mail: zhengzheng@buaa.edu.cn

Received 2 April 2013, in final form 25 May 2013
Published 29 July 2013
Online at stacks.iop.org/JPhysD/46/335102

Abstract
Hybrid dielectric-loaded plasmonic waveguide consisting of an inverted U-shaped high-index ridge covering atop a low-index polymer coated metal nanorod is proposed and numerically investigated. Through incorporating a gain medium either in the ridge or the buffer layer, the loss of the supported plasmonic mode can be effectively compensated. For a typical configuration comprising a 450 nm × 160 nm InGaAsP ridge with a 5–40 nm thick PMMA layer and a 30 nm wide Ag nanorod, the necessary gain required in InGaAsP for lossless propagation of the quasi-TE type symmetric hybrid mode can be as low as 3.45–9.85 cm^{-1}, along with a subwavelength mode area ($\lambda^2/60$–$\lambda^2/148$) attainable simultaneously. The configuration potentially offers a promising solution to enable lossless light transport at the sub-diffraction-limited scale with low compensation gain, thereby opening venues for ultra-compact active plasmonic devices and circuits.

(Some figures may appear in colour only in the online journal)

1. Introduction

Surface plasmon polariton (SPP) has attracted significant attention in recent years as an emerging field in nanophotonics owing to its remarkable capability to guide, confine and manipulate light well beyond the fundamental diffraction limit [1]. During the past decade, extensive efforts have been devoted to the design and demonstration of numerous SPP-based waveguides and components [2]. Since increasing the packing density of photonic integrated circuits is one of the ultimate goals in many of the current studies, guiding light at the subwavelength scale is highly desired. However, the huge intrinsic loss in metal has prohibited the practical implementations of many plasmonic structures. Such a problem would be further exacerbated when the mode size rapidly decreases to a sub-diffraction-limited level, with the corresponding propagation distance greatly shortened [3, 4].

In order to overcome the above limitations in conventional SPP structures, several approaches involving different waveguiding configurations have been presented. Among them, the dielectric-loaded SPP (DLSPP) [5, 6] and hybrid plasmonic (HP) waveguides [7–24] have been shown to offer good solutions in balancing the modal loss and field confinement. Although a number of related works have succeeded in demonstrating low-loss light guiding with subwavelength mode size [9, 19], the attenuation of

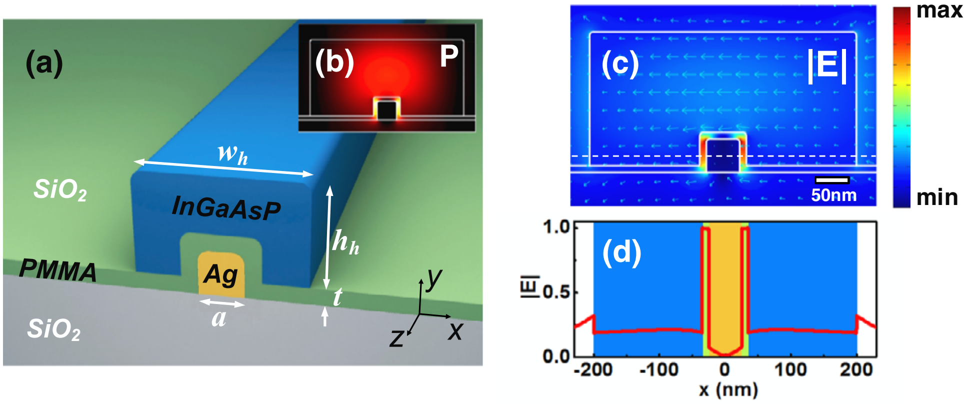

Figure 1. (*a*) Schematic diagram of the studied HDLSPPW, consisting of a square Ag nanorod (side-width: *a*) covered subsequently by a PMMA layer (thickness: *t*) and a InGaAsP ridge (width: w_h, height: h_h); (*b*) field map of 2D power flow of the quasi-TE symmetric HP mode, with parameters chosen as: $w_h = 400$ nm, $h_h = 200$ nm, $a = 50$ nm and $t = 10$ nm; (*c*) 2D electric field plot of the considered plasmonic mode. The arrows reveal the orientation of the electric field; (*d*) the corresponding 1D electric field distribution along the white dashed line in the 2D panel.

the plasmonic mode still exists due to the damping of electromagnetic fields in the metal. An attractive solution to address this challenge is by incorporating gain medium into the structure, such that the modal loss can be compensated to a certain extent. Through choosing an appropriate gain material by means of stimulated emission [25, 26], complete compensation of the modal loss can be realized, thus enabling lossless light propagation through the waveguide.

Despite the fact that a number of guiding strategies had been put forward recently to achieve the goal of loss compensation [26–32], the simultaneous realization of subwavelength field confinement with low required material gain coefficient for lossless propagation of the lightwaves has been out of reach. Previous studies regarding active HP waveguides have proposed to leverage metal-ridge-like structures to achieve nanoscale confinement [28], but the gain required for lossless propagation is relatively high (around hundreds to several thousands of cm^{-1}), which is due to the substantially increased field strength in the metallic component. On the other hand, adopting a metal stripe coupled to infinitely wide silicon layer could simplify the fabrication process and meanwhile result in significantly reduced critical material gain [30]. Yet its mode size is approaching several hundreds of nanometres, comparable to the conventional DLSPPW counterparts.

Here in this paper, we propose and investigate a novel active hybrid dielectric-loaded-type surface plasmon polariton waveguide (HDLSPPW) based on a metal nanorod. The metallic nanorod along with the nearby high-index dielectric ridge provides a unique scheme to guide and confine light into the ridge and the low-index gap surrounding the rod with low modal loss. The relatively simple and compact structure could be realized using standard fabrication processes, e.g. deposition combined with patterning/etching steps. Besides, the metal nanorod on the substrate also allows straightforward connection with external electrodes, which facilitates electro-optic control and other applications, thus maintaining the key advantages of DLSPPWs. In the following, we will carry out detailed investigations on the guiding properties of the plasmonic waveguide at the telecom wavelength. Through incorporating gain medium into the dielectric layers of the waveguide, the possibility of effectively compensating the loss of the guided mode will be further demonstrated.

2. Analysis of the proposed hybrid DLSPPW

The geometry of the studied DLSPPW is schematically shown in figure 1(*a*), where a square-shaped silver nanorod supported by a silica substrate is covered subsequently by a thin PMMA buffer and a high-index rectangular InGaAsP ridge. The metallic nanorod and the InGaAsP ridge are supposed to be located at the centre position with respect to the horizontal axis. The side-width of the square Ag nanowire is *a*, whereas the thicknesses of the PMMA layer is *t*. The InGaAsP ridge has a width of w_h and a height of h_h. For the presented configuration, gain medium can be either incorporated in the upper loaded high-index layer or low-index buffer. The pump light may be incident either from the cladding or the substrate to excite the gain material.

Simulation results reveal that the proposed dielectric-loaded plasmonic waveguide can support several plasmonic modes under a wide range of geometric parameters. In the following studies, we look into the characteristics of the quasi-TE-like symmetric HP mode, as it offers the capability of simultaneously achieving low propagation loss and subwavelength mode confinement. In figures 1(*b*)–(*d*), the power flow and the electric field distributions of the supported quasi-TE symmetric HP mode for a typical configuration are depicted, whose geometric parameters are chosen as: $w_h = 400$ nm, $h_h = 200$ nm, $a = 50$ nm and $t = 10$ nm. Owing to the high refractive index contrast near the metallic structure, pronounced local electric field enhancements can be observed inside the PMMA gap regions on both sides of the Ag nanorod (see figures 1(*c*) and (*d*)), which is similar to the HP [8] or conductor-gap-dielectric [11] waveguiding counterparts. The field map of the power flow shown in figure 1(*b*) along with the calculation of the power ratio reveal that a large portion of the mode power (∼62%) can be stored inside the

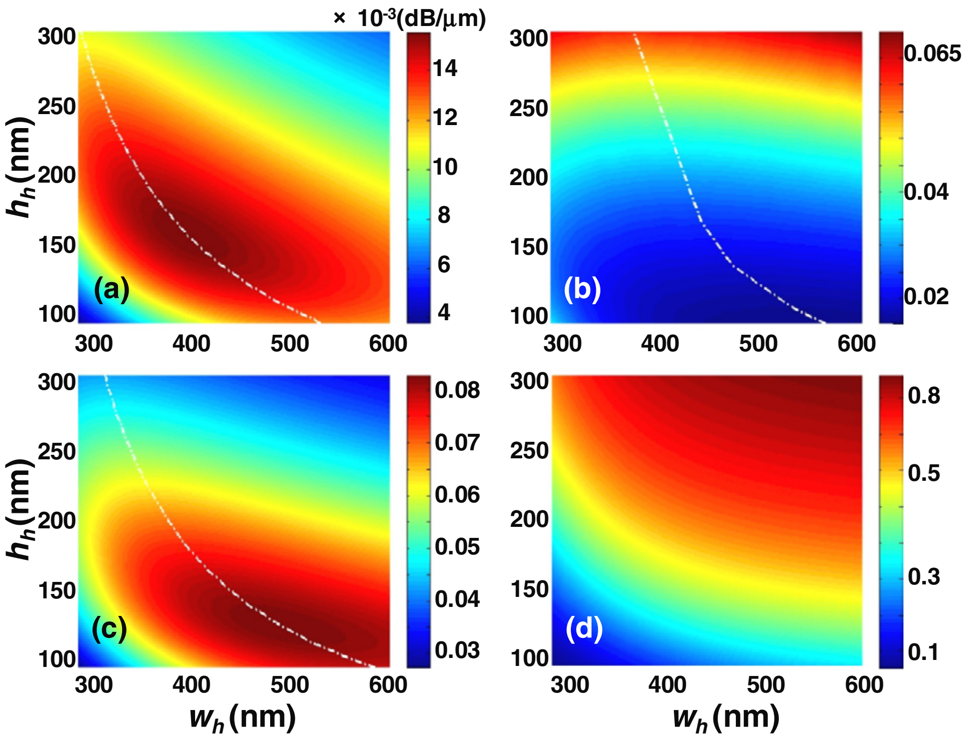

Figure 2. Dependence of modal properties on the size of the InGaAsP ridge ($t = 10$ nm, $a = 50$ nm): (*a*) propagation loss (Loss); (*b*) normalized mode area (A_{eff}/A_0); (*c*) confinement factor in the PMMA layer (Γ_{PMMA}); (*d*) confinement factor inside the InGaAsP ridge ($\Gamma_{InGaAsP}$). Dashed–dotted lines in (*a*) and (*c*) represent maximum Loss and Γ_{PMMA} for each height, while corresponding to the minimum mode area at a specific h_h in (*b*).

InGaAsP ridge. On the other hand, despite the significant field enhancement in the gap, the power ratio resided in the PMMA layer is still limited (∼7%) due to the relatively small dimension of the gap region.

To gain a comprehensive understanding of the optical behaviours, we first investigate the dependence of the quasi-TE symmetric hybrid mode's properties on the waveguide's key geometric parameters at $\lambda = 1.55\,\mu$m using the finite element method by COMSOL Multiphysics 3.5a. The permittivities of InGaAsP, Ag, PMMA and SiO_2 are $\varepsilon_h = 11.38$, $\varepsilon_m = -129 + 3.3i$ [8], $\varepsilon_l = 2.25$ and $\varepsilon_s = \varepsilon_c = 2.25$, respectively. It is notable that the high-index ridge can be made of other high-index materials as well, such as Si [29, 30] and GaAs [8, 33], while low-index material can be other polymers or silica incorporating quantum dots (QDs) nanocrystals [26] or dye molecules [25]. The propagation loss is calculated by Loss $= 8.686 \times 2\pi/\lambda \times \mathrm{Im}(N_{eff})$ (dB μm^{-1}), where N_{eff} is the complex effective index of the considered plasmonic mode obtained from the 2D eigenmode solver. $N_{eff} = k/k_0$, where k and $k_0 = 2\pi/\lambda$ are the propagation constants of the hybrid mode and the free space wave number, respectively. The effective mode area is calculated using $A_{eff} = \iint W(r)\,\mathrm{d}A/\max(W(r))$ [8]. In order to accurately account for the energy in the metal region, the electromagnetic energy density $W(r)$ is defined as

$$W(r) = \frac{1}{2}\mathrm{Re}\left\{\frac{\mathrm{d}[\omega\varepsilon(r)]}{\mathrm{d}\omega}\right\}|E(r)|^2 + \frac{1}{2}\mu_0|H(r)|^2. \quad (1)$$

In equation (1), $E(r)$ and $H(r)$ are the electric and magnetic fields, $\varepsilon(r)$ is the electric permittivity and μ_0 is the vacuum magnetic permeability. A_0 is the diffraction-limited mode area in free space and defined as $\lambda^2/4$. The confinement factor is the ratio of the power inside the considered region to the total power in the overall waveguide.

As seen in figure 2, for a fixed h_h, increasing the width of the ridge has resulted in non-monotonic trends in Loss, A_{eff} and Γ_{PMMA}. Near the strongest coupling between the high-index InGaAsP ridge and the metal nanorod, the mode exhibits significant hybrid features, which corresponds to a relatively large modal loss and a small effective mode area, along with a near-optimized optical power resided in the low-index PMMA gap, similar to many other previously studied hybrid counterparts [8, 18, 24]. Due to the fact that the area of the PMMA layer is quite small, the maximum value of the power ratio inside the gap is still limited. However, the confinement in the PMMA gap can be significantly improved through further increasing the physical dimension of the gap region, which will be discussed in the following studies. Here it is also worth noting that, this HP mode could exist for a wide geometric parameter range, even when the corresponding InGaAsP ridge by itself does not support a guided dielectric mode. In these cases, the index contrast plays a dominant role in confining the optical field and resulting in the local field enhancement. The supported plasmonic mode here behaves like a gap mode, similar to those in the conductor-gap-dielectric waveguides [11, 21]. In contrast to the non-monotonic trends of Loss, A_{eff} and Γ_{PMMA}, $\Gamma_{InGaAsP}$ exhibits a monotonic change as the ridge size increases. It is illustrated in figure 2 that for the configuration with the minimum mode area (dashed–dotted lines in (*b*)), the corresponding loss can still be deemed

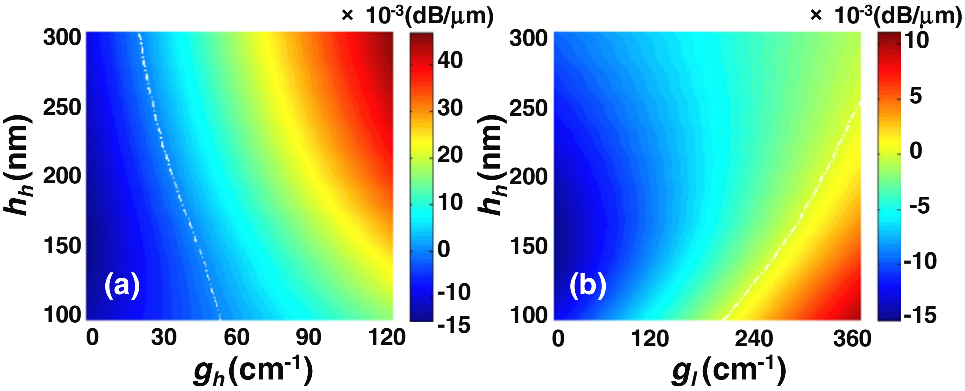

Figure 3. Dependence of gain or loss for the hybrid mode with minimum effective mode area on gain coefficient when gain is introduced in (*a*) InGaAsP and (b) PMMA layer. Note that the width of the InGaAsP ridge (w_h) for the considered structures can be read from the dashed lines in figure 2(*b*), which corresponds to the smallest mode area for each fixed h_h. White dashed–dotted lines correspond to the critical condition, enabling lossless propagation of the considered plasmonic mode.

moderate (0.009–0.015 dB μm^{-1}), which would be beneficial to enable lossless light transmission at the subwavelength with low compensation gain.

By choosing configurations with the smallest mode area along the dashed–dotted line shown in figure 2(*b*), we attempt to compensate loss through incorporating gain medium into either the InGaAsP ridge or the PMMA layer. Here, it is assumed that, the real part of the refractive index of InGaAsP or PMMA remains unchanged when gain is introduced. This assumption has also been widely employed in the studies of many other gain-assisted plasmonic waveguiding counterparts [28–30, 34]. The gain coefficient of InGaAsP (g_h) or PMMA (g_l) is written in terms of the imaginary part of its refractive index (N_g), i.e. $g_h(g_l) = 2 \times 2\pi/\lambda \times \mathrm{Im}(N_g)$ [30]. It is noted that for more accurate calculation, the Lorentz model should be adopted to determine the refractive index of QDs-doped PMMA [35] instead of the constant imaginary part assumed in our studies. In this paper, the above simple approximation has been adopted for its simplicity to illustrate the physical dimensions' influence on the waveguide's properties rather than predict the accurate gain threshold.

The resultant overall loss or gain for the mode is shown in figure 3 under various gain coefficients. It is clear that the introduced gain effectively enables partial or full compensation of the modal loss. The large magnitude of this effect can even result in net optical gain. Due to the relatively large modal overlap with the InGaAsP ridge, the gain needed for lossless propagation of the mode is relatively low, being about 20.2–52.6 cm^{-1} for the considered h_h range. Here the critical condition for lossless propagation corresponds to $\mathrm{Im}(N_{eff}) = 0$. By contrast, if gain is introduced in PMMA, lossless propagation would require a relatively larger coefficient, typically more than 192.5 cm^{-1} while over 365 cm^{-1} when the height of the waveguide exceeds ~250 nm. In the following, we will show that such a gain coefficient could be further reduced through engineering other geometric parameters.

For a fixed InGaAsP ridge, the size of the metallic nanorod and the thickness of the PMMA layer also exert great impact on the overall modal behaviours, which might be leveraged as additional freedom to balance gain and mode area. In the following investigations, the size of the InGaAsP is fixed at 450 nm × 160 nm to ensure both small mode area and moderate propagation loss, whereas a is varied from 30 to 210 nm and t is tunable within the range 5–40 nm. As shown in figures 4(*a*)–(*d*), increasing the size of the nanorod results in increased Loss, reduced A_{eff} and smaller $\Gamma_{InGaAsP}$. While reduced modal loss and decreased $\Gamma_{InGaAsP}$, along with increased A_{eff} can be observed when the PMMA layer gets thicker. In contrast, Γ_{PMMA} demonstrates different trends for different configurations. Monotonic increase of Γ_{PMMA} is observable when both a and t are small, while non-monotonic changes take place as the nanorod and PMMA layer get larger. Corresponding to these modal behaviours, the trend of material gain needed for lossless propagation may be also explained. Small compensation gain coefficient is realizable only when low modal loss and high power ratio in the gain medium can be achieved simultaneously. As shown in figures 4(*e*)–(*f*), low material gain is sufficient to fully compensate loss when the nanorod is small. For the case of $a = 30$ nm, the critical material gain can be as low as 3.45–9.85 cm^{-1} and 27.4–177.3 cm^{-1} in InGaAsP and PMMA, respectively, along with a subwavelength mode area ($\lambda^2/60$–$\lambda^2/148$). These values suggest that currently available InGaAsP gain medium [36, 37] and QDs-doped PMMA [26] could provide enough gain for lossless or nearly lossless propagation of the HP modes. Besides, the mode size can be further reduced by adopting other configurations. For instance, a deep-subwavelength mode area of $\lambda^2/381$ can be achieved in a waveguide with $a = 90$ nm and $t = 5$ nm. While for such case a moderate gain coefficient of ~302.5 cm^{-1} in InGaAsP is sufficient for lossless propagation.

To provide further comparison with the performance of conventional hybrid plasmonic waveguide (HPW), we here introduce a 2D parameter plot of material gain versus normalized mode area [8]. As shown in figure 5, both waveguides can achieve lossless propagation with moderate material gain and small mode size. For HDLSPPW, the material gain required in InGaAsP for lossless light transport can be more than two orders of magnitude smaller than that of the HPW case, with a subwavelength mode area

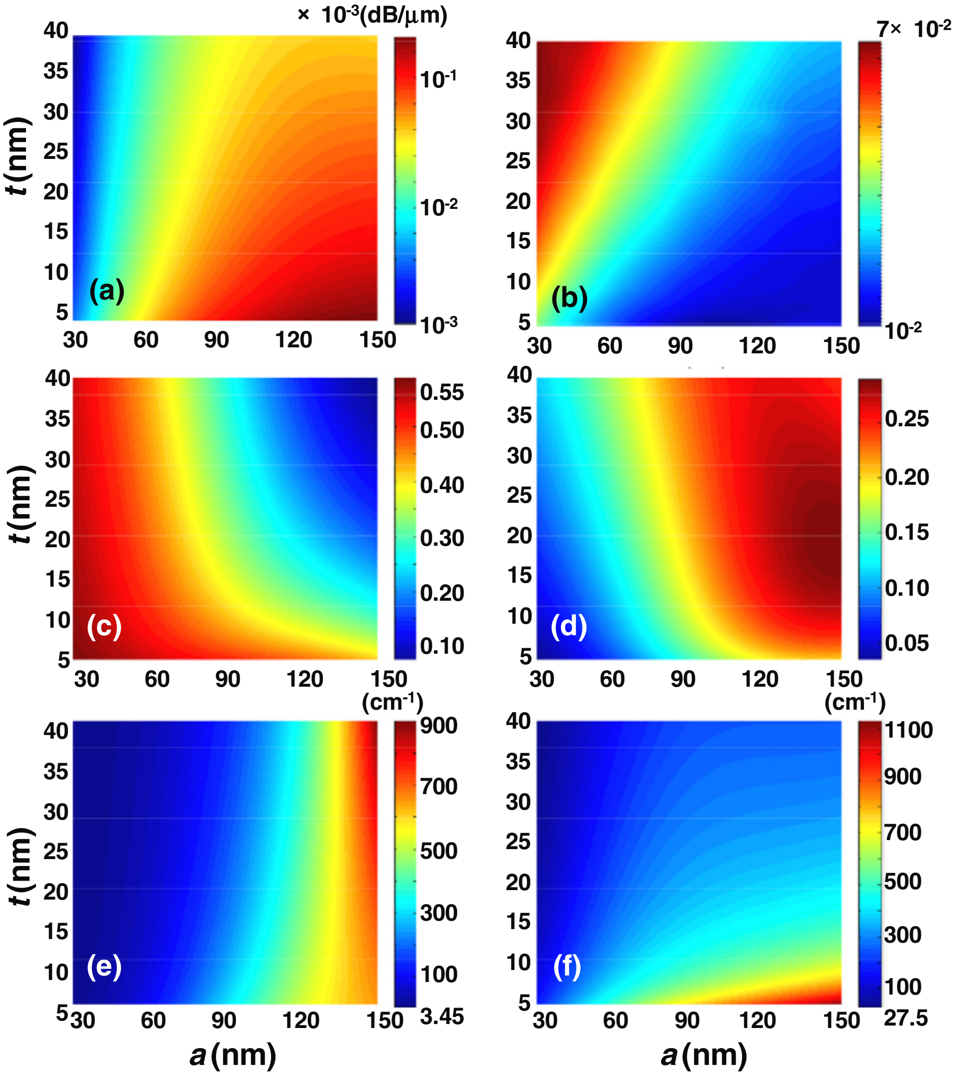

Figure 4. (*a*)–(*d*) Dependence of modal properties on the dimensions of the Ag nanorod and PMMA layer ($w_h = 450$ nm, $h_h = 160$ nm): (*a*) propagation loss (Loss); (*b*) normalized mode area (A_{eff}/A_0); (*c*) confinement factor inside InGaAsP ($\Gamma_{InGaAsP}$); (*d*) confinement factor in PMMA (Γ_{PMMA}). (*e*)–(*f*) Material gain required for lossless propagation (g_m) when gain is incorporated in InGaAsP layer (*e*) and PMMA layer (*f*).

achieved simultaneously. On the other hand, for the PMMA case shown in figure 5(*b*), using HDLSPPW instead of HPW, the critical gain coefficient can be reduced nearly one order of magnitude while still retaining subwavelength field confinement. For both of the above cases, by choosing appropriate configurations, much lower critical material gain is required for the proposed HDLSPPW than that needed in the standard HPW for similar degrees of confinement. For example, considering a HDLSPPW with $a = 30$ nm and $t = 40$ nm, the normalized mode area is 0.07, while the critical material gains for lossless propagation are $g_m = 3.45\,\text{cm}^{-1}$ for InGaAsP and $g_m = 27.4\,\text{cm}^{-1}$ for PMMA. By contrast, for the corresponding HPW with the same gap size ($t = 40$ nm), its normalized mode area is 0.058, which is slightly smaller than that of the HDLSPPW. However, the critical material gain coefficients are much larger than those required for HDLSPPW, which are $g_m = 601.3\,\text{cm}^{-1}$ for InGaAsP and $g_m = 266.8\,\text{cm}^{-1}$ for PMMA. These results reveal the possibility of further improving the optical performance of the conventional active HPWs through employing the presented HDLSPPW structures.

An important issue that should be addressed in practical applications of the proposed active HDLSPPW is the effect of the non-uniform spatial profile of the deposited gain on the loss compensation efficiency upon optical pumping [38]. It is also worth mentioning that, in addition to the widely employed loss compensation methods using gain media as studied in this paper, the recently presented approaches for significant reduction of the propagation losses in metal-coated nanofibers [39] or multilayer planar metallic waveguides [40] might be considered as intriguing alternatives to minimize the modal loss of HDLSPPW. To make the latter approach work effectively for the proposed structure, a major challenge to overcome is the greatly weakened field confinement associated with the rapidly extended propagation distance, as seen in the previously demonstrated plasmonic waveguides supporting ultra-long-range SPPs [40]. Therefore, more careful designs with consideration of both the existence condition of the ultra-long-range plasmonic modes and the maintenance of

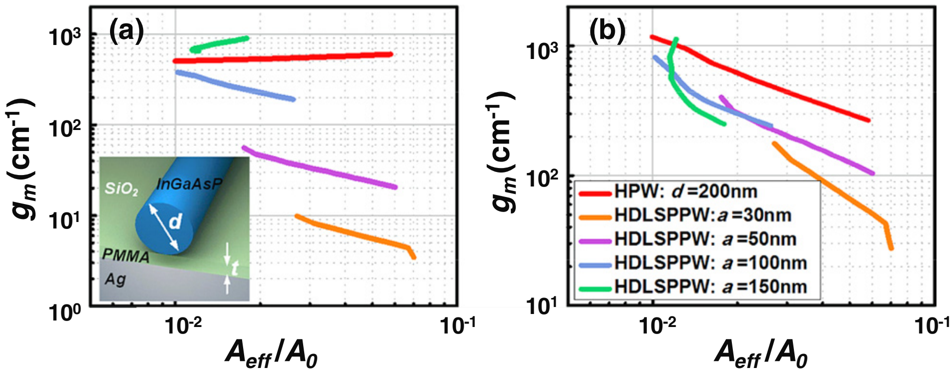

Figure 5. Performance comparison between HDLSPPW (w_h = 450 nm, h_h = 160 nm, t: 5–40 nm) and conventional HPW (t: 5–40 nm): (*a*) gain introduced in InGaAsP, where the inset illustrates the geometry of the conventional HPW; (*b*) gain incorporated in PMMA.

the subwavelength field confinement capability are required, which may be the focus of our future study.

3. Conclusions

In conclusion, we have investigated an active HDLSPPW for lossless light propagation with low compensation gain and subwavelength mode size. The critical material gain of the presented HDLSPPW can be much smaller than that of the conventional HPW while maintaining a comparable tight field confinement. The nice optical performance of the studied HDLSPPW could enable potential applications in compact active components and circuits.

Acknowledgments

The work at Beihang University was supported by 973 Program (2009CB930702), NSFC (61221061/61077064), National key scientific instruments and equipment development special fund management (2011YQ0301240502) and Scholarship Award for Excellent Doctoral Student granted by Ministry of Education. The authors would like to acknowledge Professor Yunfeng Xiao in Department of Physics, Peking University for fruitful discussions.

References

[1] Barnes W L, Dereux A and Ebbesen T W 2003 Surface plasmon subwavelength optics *Nature* **424** 824–30
[2] Gramotnev D K and Bozhevolnyi S I 2010 Plasmonics beyond the diffraction limit *Nature Photon.* **4** 83–91
[3] Liu L, Han Z and He S 2005 Novel surface plasmon waveguide for high integration *Opt. Express* **13** 6645–50
[4] Krasavin A V and Zayats A V 2011 Guiding light at the nanoscale: numerical optimization of ultrasubwavelength metallic wire plasmonic waveguides *Opt. Lett.* **36** 3127–9
[5] Holmgaard T and Bozhevolnyi S I 2007 Theoretical analysis of dielectric-loaded surface plasmon-polariton waveguides *Phys. Rev.* B **75** 245405
[6] Krasavin A V and Zayats A V 2007 Passive photonic elements based on dielectric-loaded surface plasmon polariton waveguides *Appl. Phys. Lett.* **90** 211101
[7] Oulton R F, Sorger V J, Zentgraf T, Ma R M, Gladden C, Dai L, Bartal G and Zhang X 2009 Plasmon lasers at deep subwavelength scale *Nature* **461** 629–32
[8] Oulton R F, Sorger V J, Genov D A, Pile D F P and Zhang X 2008 A hybrid plasmonic waveguide for subwavelength confinement and long-range propagation *Nature Photon.* **2** 496–500
[9] Sorger V J, Ye Z, Oulton R F, Wang Y, Bartal G, Yin X and Zhang X 2011 Experimental demonstration of low-loss optical waveguiding at deep sub-wavelength scales *Nature Commun.* **2** 331
[10] Alam M Z, Meier J, Aitchison J S and Mojahedi M 2010 Propagation characteristics of hybrid modes supported by metal-low-high index waveguides and bends *Opt. Express* **18** 12971–9
[11] Avrutsky I, Soref R and Buchwald W 2010 Sub-wavelength plasmonic modes in a conductor-gap-dielectric system with a nanoscale gap *Opt. Express* **18** 348–63
[12] Bian Y S, Zheng Z, Zhao X, Zhu J S and Zhou T 2009 Symmetric hybrid surface plasmon polariton waveguides for 3D photonic integration *Opt. Express* **17** 21320–5
[13] Chu H S, Bai P, Li E P and Hoefer W R J 2011 Hybrid dielectric-loaded plasmonic waveguide-based power splitter and ring resonator: compact size and high optical performance for nanophotonic circuits *Plasmonics* **6** 591–7
[14] Fang Z Y, Qi H, Wang C and Zhu X 2010 Hybrid plasmonic waveguide based on tapered dielectric nanoribbon: excitation and focusing *Plasmonics* **5** 207–12
[15] Bian Y S, Zheng Z, Liu Y, Liu J S, Zhu J S and Zhou T 2011 Hybrid wedge plasmon polariton waveguide with good fabrication-error-tolerance for ultra-deep-subwavelength mode confinement *Opt. Express* **19** 22417–2
[16] Kim J T 2011 CMOS-compatible hybrid plasmonic waveguide for subwavelength light confinement and on-chip integration *IEEE Photon. Technol. Lett.* **23** 206–8
[17] Kwon M S 2011 Metal–insulator–silicon–insulator–metal waveguides compatible with standard CMOS technology *Opt. Express* **19** 8379–93
[18] Bian Y S, Zheng Z, Zhao X, Su Y L, Liu L, Liu J S, Zhu J S and Zhou T 2012 Guiding of long-range hybrid plasmon polariton in a coupled nanowire array at deep-subwavelength scale *IEEE Photon. Technol. Lett.* **24** 1279–81
[19] Zhu S Y, Liow T Y, Lo G Q and Kwong D L 2011 Fully complementary metal-oxide-semiconductor compatible nanoplasmonic slot waveguides for silicon electronic photonic integrated circuits *Appl. Phys. Lett.* **98** 021107
[20] Lu C C, Hu X Y, Song Y, Fu Y L, Yang H and Gong Q H 2013 Ferroelectric hybrid plasmonic waveguide for all-optical logic gate applications *Plasmonics* **8** 749–54
[21] Wu M, Han Z H and Van V 2010 Conductor-gap-silicon plasmonic waveguides and passive components at subwavelength scale *Opt. Express* **18** 11728–36

[22] Chu H S, Li E P, Bai P and Hegde R 2010 Optical performance of single-mode hybrid dielectric-loaded plasmonic waveguide-based components *Appl. Phys. Lett.* **96** 221103

[23] Bian Y S, Zheng Z, Zhao X, Su Y L, Liu L, Liu J S, Zhu J S and Zhou T 2013 Highly confined hybrid plasmonic modes guided by nanowire-embedded-metal grooves for low-loss propagation at 1550 nm *IEEE J. Sel. Top. Quantum Electron.* **19** 4800106

[24] Bian Y S, Zheng Z, Zhao X, Liu L, Su Y L, Liu J S, Zhu J S and Zhou T 2013 Dielectrics covered metal nanowires and nanotubes for low-loss guiding of subwavelength plasmonic modes *J. Light. Technol.* **31** 1973–9

[25] Noginov M A, Zhu G, Belgrave A M, Bakker R, Shalaev V M, Narimanov E E, Stout S, Herz E, Suteewong T and Wiesner U 2009 Demonstration of a spaser-based nanolaser *Nature* **460** 1110–2

[26] Grandidier J, Francs G C D, Massenot S, Bouhelier A, Markey L, Weeber J C, Finot C and Dereux A 2009 Gain-assisted propagation in a plasmonic waveguide at telecom wavelength *Nano Lett.* **9** 2935–9

[27] Garcia-Blanco S M, Pollnau M and Bozhevolnyi S I 2011 Loss compensation in long-range dielectric-loaded surface plasmon-polariton waveguides *Opt. Express* **19** 25298–310

[28] Zhang J, Cai L K, Bai W L, Xu Y and Song G F 2011 Hybrid plasmonic waveguide with gain medium for lossless propagation with nanoscale confinement *Opt. Lett.* **36** 2312–4

[29] Dai D X, Shi Y C, He S L, Wosinski L and Thylen L 2011 Gain enhancement in a hybrid plasmonic nano-waveguide with a low-index or high-index gain medium *Opt. Express* **19** 12925–36

[30] Gao L F, Tang L X, Hu F F, Guo R M, Wang X J and Zhou Z P 2012 Active metal strip hybrid plasmonic waveguide with low critical material gain *Opt. Express* **20** 11487–95

[31] He X Y, Wang Q J and Yu S F 2012 Numerical study of gain-assisted terahertz hybrid plasmonic waveguide *Plasmonics* **7** 571–7

[32] Rao R and Tang T 2012 Study of an active hybrid gap surface plasmon polariton waveguide with nanoscale confinement size and low compensation gain *J. Phys. D: Appl. Phys.* **45** 245101

[33] Galli M, Agio M, Andreani L C, Atzeni L, Bajoni D, Guizzetti G, Businaro L, Di Fabrizio E, Romanato F and Passaseo A 2002 Optical properties and photonic bands of GaAs photonic crystal waveguides with tilted square lattice *Eur. Phys. J.* B **27** 79–87

[34] Bian Y S, Zheng Z, Zhao X, Yang P F, Liu L, Zhu J S and Zhou T 2013 Gain enhancement in a V-shaped plasmonic slot waveguide for efficient loss compensation at the subwavelength scale *Opt. Commun.* **294** 414–9

[35] Kirby E I, Hamm J M, Pickering T W, Tsakmakidis K L and Hess O 2011 Evanescent gain for slow and stopped light in negative refractive index heterostructures *Phys. Rev.* B **84** 041103(R)

[36] Hill M T *et al* 2007 Lasing in metallic-coated nanocavities *Nature Photon.* **1** 589–94

[37] Nezhad M P, Simic A, Bondarenko O, Slutsky B, Mizrahi A, Feng L A, Lomakin V and Fainman Y 2010 Room-temperature subwavelength metallo-dielectric lasers *Nature Photon.* **4** 395–9

[38] Hess O, Pendry J B, Maier S A, Oulton R F, Hamm J M and Tsakmakidis K L 2012 Active nanoplasmonic metamaterials *Nature Mater.* **11** 573–84

[39] Song J F, Zaccaria R P, Dong G C, Di Fabrizio E, Yu M B and Lo G Q 2011 Evolution of modes in a metal-coated nano-fiber *Opt. Express* **19** 25206–21

[40] Adato R and Guo J 2007 Characteristics of ultra-long range surface plasmon waves at optical frequencies *Opt. Express* **15** 5008–17